OXFORD UNIVERSITY PRESS | Genome Biology and Evolution

Not All Roads Lead to Red: The genetics of sexual dichromatism in the northern cardinal (Cardinals cardinalis)

Journal:	*Genome Biology and Evolution*
Manuscript ID	GBE-260118.R1
Manuscript Type:	Article
Date Submitted by the Author:	23-Apr-2026
Complete List of Authors:	Wade, Miranda; The University of Hong Kong, School of Biological Sciences Patton, Sara; Auburn University Scheer, Elizabeth; University of Tulsa Koch, Rebecca; University of Wisconsin-Stevens Point, Biology Zhang, Yufeng; College of Health Sciences University of Memphis Toomey, Matthew; University of Tulsa; Michigan State University Hill, Geoffrey; Auburn University Sin, Simon; Harvard University, Organismic and Evolutionary Biology; The University of Hong Kong, School of Biological Sciences
Keywords:	Avian plumage color, carotenoid-based pigmentation, coloration genetics, feather coloration, sexual conflict, sexual dichromatism

Title

Not All Roads Lead to Red: The genetics of sexual dichromatism in the northern cardinal (*Cardinals cardinalis*)

Authors (ORCiDs hyperlinked)

Miranda J. Wade[1], Sara Patton[2], Elizabeth C. Scheer[3], Rebecca E. Koch[4], Yufeng Zhang[6], Matthew B. Toomey[3,5], Geoffrey E. Hill[2], Simon Yung Wa Sin[1]

Affiliations

[1]School of Biological Sciences, The University of Hong Kong, Hong Kong, China.

[2]Department of Biological Sciences, Auburn University, Auburn, AL 36849, USA.

[3]Department of Biological Science, University of Tulsa, Tulsa, OK 74104, USA.

[4]Department of Biology, University of Wisconsin-Stevens Point, Stevens Point, WI 54481.

[5]Department of Integrative Biology, Michigan State University, East Lansing, MI 48824, USA.

[6]College of Health Sciences, University of Memphis, Memphis, TN 38152, USA.

Corresponding author

Simon Yung Wa Sin

Email: sinyw@hku.hk

Abstract

Sexual dichromatism, characterized by sex-specific differences in coloration, is widespread among birds and often involves carotenoid-based pigmentation. Despite extensive research on the social and ecological environments favoring sexual dichromatism, the molecular mechanisms underlying its development and evolution remain largely unexplored. In this study, we investigated the genetic and molecular processes giving rise to sexual dichromatism in the red ketocarotenoid-based plumage coloration of northern cardinals (*Cardinalis cardinalis*). We quantified carotenoid concentrations in plasma and feather follicles, confirmed that homologs of *CYP2J19*, *BDH1L*, and *TTC39B* catalyze the addition of a keto group at C4, and performed gene expression analyses across tissues. Males showed significantly higher plasma and feather ketocarotenoid concentrations along with upregulated *CYP2J19* and *TTC39B* expression in liver and feather tissues and upregulated carotenoid transport gene expression in gut and feather follicles. Females exhibited a dramatic upregulation of *BCO2*, facilitating carotenoid degradation and attenuating red pigmentation. Additionally, sex-biased expression of hormonal regulators such as *HSD17B4* and *ZNF131* in the feather follicle suggests hormonal modulation influences dichromatism. These findings indicate that sex-specific regulation of carotenoid processing genes underpins the vivid red coloration in males and the drab phenotype in females, likely maintained by a balance between natural and sexual selection, with mechanisms of sexual antagonism effecting divergent gene expression. Our work advances understanding of the molecular basis of avian sexual dimorphism, highlighting key

genetic pathways involved in carotenoid-based coloration and providing a foundation for further research into the evolution of sexually dichromatic traits.

Keywords

Avian plumage color, carotenoid-based pigmentation, coloration genetics, feather coloration, sexual conflict, sexual dichromatism.

Significant statement

The molecular mechanisms underlying the development and evolution of sexual dichromatism involving carotenoid-based pigmentation remain largely unexplored. We explored gene expression during feather growth and show that sexual dichromatism is largely attributed to a few genes in the northern cardinal. In particular, the highly upregulated *BCO2* in developing feathers of females indicates that carotenoid breakdown is the major action leading to a reduction of red plumage color in females, while males have upregulation of *CYP2J19* and *TTC39B* in liver and feather follicles and carotenoid uptake genes in both the gut and feather follicles, suggesting that the dichromatism is maintained by both natural and sexual selection, with sexual antagonism driving divergent gene expression. These findings provide new insight into the genetic basis and evolution of avian sexual dichromatism.

Introduction

Sexual dichromatism, where sexes differ in patterning or coloration, is a common form of dimorphism seen across diverse animal taxa. In particular, birds are among the most conspicuous examples and have long been the subject of study regarding the evolution and maintenance of sexual dichromatism (Badyaev and Hill 2000; Shultz and Burns 2017). Sexual dichromatism in birds often involves carotenoid-based pigmentation. Vertebrates cannot synthesize carotenoids, so carotenoid-based pigmentation requires birds to first obtain carotenoids such as zeaxanthin and lutein from their diet. These dietary carotenoids can either be integrated directly or further modified to produce a wider range of red, orange, and yellow pigments (Hill and McGraw 2006a), however sexual dichromatism tends to be strongest in species that have red carotenoid-based coloration (Delhey and Peters 2017). Recent progress in discovering the genes involved in avian carotenoid pigmentation has created opportunities to investigate mechanistic hypotheses for the development and evolution of sexual dichromatism.

The expression of gene products mediate carotenoid uptake, binding, metabolism, deposition, and breakdown, shaping plumage coloration and patterning (Toews et al. 2017; Hill and McGraw 2006b). Genes that regulate the uptake of carotenoids in birds include scavenger receptor B1 (*SCARB1*) and scavenger receptor class F member 2 (*SCARF2*) (Brelsford et al. 2017; Toomey et al. 2017). Additionally, 3-hydroxybutyrate dehydrogenase 1-like (*BDH1L*) converts the dietary carotenoids lutein and zeaxanthin to canary xanthophylls (Toomey et al. 2022; Toomey et al. 2025), a yellow pigment in the plumage of many birds. In concert with *BDH1L*, cytochrome P450

2J19 encoded by the gene *CYP2J19* catalyzes the production of red C-4 ketocarotenoids (hereafter referred to as “ketocarotenoids”) from dietary carotenoids in many birds (Lopes et al. 2016; Mundy et al. 2016; Toomey et al. 2022; Toomey et al. 2025). Multiple studies have found that *CYP2J19* (or a homolog) contributes to red coloration in natural populations (Twyman et al. 2018; Hooper et al. 2019; Kirschel et al. 2020; Aguillon et al. 2021; Khalil et al. 2023; Ranasinghe et al. 2025), indicating that the CYP2J19/BDH1L enzymatic pathway is a widespread mechanism of ketocarotenoid synthesis in birds. Furthermore, ketocarotenoid production is enhanced by tetratricopeptide repeat protein 39B (*TTC39B*) in birds (Toomey et al. 2022; Hooper et al. 2024).

In addition to carotenoid uptake and modification, the breakdown of these pigments also contributes to avian coloration. The expression of β-carotene oxygenase 2 (*BCO2*), which catalyzes the cleavage of carotenoid molecules (Toomey et al. 2016), is linked with the loss of carotenoids in the feathers, skin, and beak of several bird species (Eriksson et al. 2008; Gazda et al. 2020b; Baiz et al. 2021; Enbody et al. 2021). In the *mosaic* breed of the domestic canary (*Serinus canaria*), the mechanism behind dichromatism lies in the selective degradation of carotenoids catalyzed by *BCO2* rather than the upregulation of red carotenoid metabolism via *CYP2J19* expression or any physiological difference in carotenoid uptake or transport (Gazda et al. 2020a). Dichromatism in yellow carotenoid coloration of plumage of European serins (*Serinus serinus*) was similarly attributed to upregulation of *BCO2* in females (Gazda et al. 2020a). Since reproductively senescent and ovariectomized female canaries develop color patterning similar to that of males (Perez-Beato 2008), *BCO2* expression may be

estrogen-dependent (Gazda et al. 2020a). In estrogen-dependent dichromatism, dull plumage develops in the presence of estrogen, while bright coloration develops in its absence (Kimball and Ligon 1999). Prior work has also found evidence for localized hormonal regulation between the sexes in birds for the hormone 17β-hydroxysteroid dehydrogenase type 4 (*HSD17B4*) in developing zebra finch (*Taeniopygia guttata*) brains (London et al. 2010; Tomaszycki and Dzubur 2013) and in their melanin-pigmented cheek patch due to sex-biased transcription factor expression (Lin et al. 2025). Steroid hormone-associated genes displaying sex-specific expression patterns have been implicated as upstream regulators influencing carotenoid-based sexual dimorphism in the toad-headed agamid lizard (*Phrynocephalus putjatai*) (Lu et al. 2024). Evidence from feather ketocarotenoid and gene expression analysis in red-backed fairywrens (*Malurus melanocephalus*) suggests that testosterone mediates plumage redness, as testosterone-implanted males had higher feather ketocarotenoid concentrations and a greater magnitude of *CYP2J19* expression compared to control males (Khalil et al. 2023). This work also reported increased expression of *BCO2* in the unornamented compared to the ornamented males. Combined, these studies suggest that divergence in ketocarotenoid metabolism and carotenoid cleavage between the sexes, perhaps due to the influence of sex-biased hormones or other regulatory factors, contributes to the development of carotenoid-based sexual dichromatism in birds.

To provide molecular insights into the development and evolution of sexual dichromatism, we quantified gene expression and carotenoid concentrations in key tissues of male and female northern cardinals (*Cardinalis cardinalis*) during their natural seasonal molt. Adult male northern cardinals possess iconic bright red plumage and

bills pigmented with carotenoids (McGraw, Hill, et al. 2003; Patton et al. 2026). Adult females largely lack red coloration in their body plumage and have orange bills, making them much drabber than males. However, females have some red coloration on their crests, underwing coverts, and flight and tail feathers (Figure 1). The pigments used by northern cardinals to color both feathers and bills are derived by modifying yellow dietary carotenoids to produce red ketocarotenoids (Patton et al. 2026). Prior analysis shows that the red feathers of male northern cardinals contain the ketocarotenoids α-doradexanthin, astaxanthin, canthaxanthin, and adonirubin (McGraw et al. 2001; McGraw, Hill, et al. 2003; Toomey et al. 2022). Since both α-doradexanthin and astaxanthin are produced by the action of *CYP2J19*, *BDH1L*, and *TTC39B* in other bird species (Toomey et al. 2022), we hypothesized that homologs of these genes from northern cardinals have the same function in ketocarotenoid production and performed cell-based assays to confirm this mechanism. As the tissue location of ketocarotenoid metabolism in birds seems to vary both by species and mechanism (Hill and McGraw 2006a; Alonso-Alvarez et al. 2022), we investigated carotenoid concentrations in plasma and feather follicles in conjunction with gene expression analysis. We hypothesized that carotenoid metabolism occurs in the liver and feather follicle of northern cardinals and that males would have higher plasma and feather follicle concentrations of ketocarotenoids and canary xanthophylls compared to females. Based on the research outlined above, we also hypothesized that male northern cardinals would have an accompanying greater transcription of the genes *CYP2J19, TTC39B,* and *BDH1L,* whereas females would have higher transcription of *BCO2*. The differences in the carotenoid coloration of males and females appear to be partly under

localized control; observations of a bilateral gynandromorph northern cardinal (Peer and Motz 2014), a chimera of male and female that display the typical plumage color of each sex on each half of the body, suggests the role of localized factors in controlling plumage color. Thus, we analyzed gene expression in the gut, liver, and feather follicle to investigate if genes related to carotenoid uptake, transport, metabolism, and deposition, along with hormone-related genes, show a sex-biased expression pattern and therefore contribute towards sexual dichromatism.

Results

Male cardinals circulate and deposit more ketocarotenoids in their plasma and feathers than females

The plasma concentrations of dietary carotenoids (i.e. lutein and zeaxanthin), canary xanthophylls, and non-ketocarotenoids were similar between the male and female northern cardinals (Figures 2A, 2C, 2E, 2G; Supplementary Table S1). However, the plasma concentration of ketocarotenoids was significantly higher in males than females ($p<0.01$), with a mean concentration of 20.01 μg mL^{-1} in the males and 8.65 μg mL^{-1} in the females (Figure 2A). In the sexually dichromatic breast feather follicles, concentrations of canary xanthophylls, non-ketocarotenoids, and ketocarotenoids, but not dietary carotenoids, were significantly different between male and female northern cardinals (Figures 2B, 2D, 2F, 2H; Supplementary Table S1). The average concentration of canary xanthophylls present in the males was 10.7 μg mg^{-1}, which was significantly greater than the average of 0.23 μg mg^{-1} in the females ($p<0.001$, Figure 2H). The average concentration of non-ketocarotenoids was 0.34 μg mg^{-1} and 5.14 μg mg^{-1} in the females and males, respectively ($p<0.001$, Figure 2D). For ketocarotenoids, the mean concentration measured in the females was 10.64 μg mg^{-1} whereas that in the males was significantly higher at 125.7 μg mg^{-1} ($p<0.001$ Figure 2B). We also found that the concentration of circulating ketocarotenoids correlated significantly (Pearson's product-moment correlation, r=0.71, $p<0.001$) with the ketocarotenoid concentration of the feather follicles.

A shared pathway for ketocarotenoid metabolism

Consistent with our hypothesis of conserved biochemical function of carotenoid metabolizing gene products, heterologous expression assays confirm that the co-expression of the northern cardinal homologs of *BDH1L*, *CYP2J19*, and *TTC39B* are sufficient to catalyze the conversion of yellow dietary carotenoids into red ketocarotenoids (Figure 3). We confirmed the formation of astaxanthin in the cells given zeaxanthin (Figure 3, top) or of α-doradexanthin in the cells provided lutein (Figure 3, bottom) as substrate. Thus, the expression of the northern cardinal homologs of *BDH1L*, *CYP2J19*, and *TTC39B* is sufficient to produce the red ketocarotenoid pigments that are enriched in the plasma and feather follicles of male cardinals. Therefore, we hypothesized that sexual dimorphism in red coloration is driven, at least in part, by differences in the expression of these genes between male and female cardinals.

Male cardinals had increased transcription of genes involved in ketocarotenoid metabolism and carotenoid transport across tissues

We compared gene expression in the feather follicles, gut, and liver of wild-caught molting male and female cardinals using RNA sequencing. We found 775 differently expressed genes (DEGs) between the male and female cardinals in the breast feather follicle (Figure 4A, Supplementary Table S4). In the liver and gut tissue, we found a total of 116 and 298 DEGs between the two sexes, respectively (Figure 4C and 4D, Supplementary Tables S5 and S6). In the feather follicles, 328 genes were upregulated in the males, including *TTC39B* (LFC=-1.36, adj-*p*=1.26E-07; Figure 4A & 5B). However, we did not find an accompanying, significant difference in the expression

of *CYP2J19* (LFC=-0.47, adj-*p*=0.2, Figure 4A and 5A) between the sexes in this tissue. In fact, female and male cardinals had similar expression in *CYP2J19* in their feather follicles quantified as transcripts per million (TPM; Figure 5A). In contrast, in the liver we found *CYP2J19* was significantly enriched in males (LFC=-2.44, adj-*p*=0.01, Figure 4D & 5A) but there were no significant differences in *TTC39B* expression (LFC=-0.59, adj-*p*=0.35). Interestingly, we found that the third gene playing a key role in converting dietary carotenoids into ketocarotenoids, *BDH1L,* was expressed at similar levels in both males and females (Figure 5C), suggesting that *BDH1L* is not a gene contributing to sexual dichromatism in northern cardinals. While *BDH1L* is expressed at a higher level in the liver than in feather follicles in both sexes (average expression in the liver=66.2 TPM, feather follicle average=34.8 TPM, *p*=0.003), *CYP2J19* is expressed at a much higher level in feather follicles than in liver tissue (average expression in the liver=5.3 TPM, feather follicle average=121.3 TPM, *p*=1.46E-11). As the average expression levels for *CYP2J19* inclusive of both sexes is 121.26 TPM in the feather follicles and 5.26 TPM in the liver, there is an almost 24-fold difference in transcription (Figure 5A).

We found expression changes in other genes encoding several lipid transport-related proteins. Interestingly, we did not find evidence of the enrichment for the known carotenoid uptake gene *SCARB1* (Toomey et al. 2017) in the males. However, Solute Carrier Family 27 Member 6 (*SLC27A6*, LFC=-1.48, adj-*p*=3.91E-08) was upregulated in the feather follicles of males (Figure 4A). *SLC27A6* is involved in the transport, formation, and secretion of chylomicrons, which are integral in the uptake and transportation of dietary carotenoids (Lee et al. 1999; Hill and Johnson 2012; Nishida et

al. 2023). We also found increased transcription of perilipin 2 (*PLIN2*, LFC=-0.79, p=0.01) in male feather follicles. *PLIN2* encodes a structural protein involved in the formation and stabilization of lipids that transport hydrophobic molecules like carotenoids (Liu et al. 2021). Both *SLC27A6* (LFC=-1.02, adj-*p*=0.0002) and *PLIN2* (LFC=-0.73, adj-*p*=0.009) were also upregulated in the gut tissues of males (Figure 4C), suggesting that these genes may increase carotenoid absorption from food contents to the bloodstream. Cluster-determinant 36 (*CD36*), similarly involved in carotenoid uptake and transportation (Liu et al. 2023), was upregulated in male feather follicles (LFC=-1.1, p=0.02; Figure 4A).

Females appear to moderate ketocarotenoid pigmentation by upregulating BCO2 expression

In the liver and gut tissues, we found no carotenoid-related genes in the 17 and 45 genes that were upregulated in females, respectively (Figures 4C & 4D, Supplementary Tables S5 and S6). In the breast feather follicles, we found 447 genes upregulated in the females (Supplementary Table S4). In particular, *BCO2* was highly upregulated in the females compared to the males (Figures 4A & 5D). This differential expression of *BCO2* was also highly significant, with over eight-hundred-fold greater transcript levels in females (adj-*p*=8.62E-102; LFC=9.65; Figures 4B & 5D). Across our analyses, *BCO2* had both the highest LFC and most significant *p*-value for its differential expression between the sexes. *BCO2* codes for an enzyme that plays a key role in carotenoid degradation by catalyzing the 9',10' oxidative cleavage of carotenoids

to yield shorter apocarotenoids (Dela Seña et al. 2016; Ahi et al. 2020; Gazda, et al. 2020a; Gazda, et al. 2020b).

Differential melanin synthesis in feathers also contributes to sexual dichromatism

Several genes involved in melanin-based pigmentation were upregulated in females (Figure 4A). These genes included Tyrosinase (*TYR*, LFC=1.98, adj-*p*=3.7e-07), responsible for catalyzing the rate-limiting step of melanogenesis (Hubbard et al. 2010), Major Facilitator Superfamily Domain Containing 12 (*MFSD12*, LFC=1.45, adj-*p*=2.3e-13), which is essential in importing cysteine into melanosomes (Adelmann et al. 2020), and tyrosinase-related protein 1 (*TYRP1,* LFC=1.05, adj-*p*=0.02), which is involved in melanin deposition in many vertebrates (Lyons et al. 2005; Chen et al. 2021; Melo-Rojas et al. 2023). In the female feather follicles also found increased transcription in the melanocortin-1 receptor (*MC1R*, LFC=0.96, adj-*p*=0.001), which has a diverse role in patterning across species and serves as a regulator of *TYR* (Mundy 2005; Bourgeois et al. 2012; Yan et al. 2022), and ocular albinism type 1 (*OA1/GPR143,* LFC=0.69, adj-*p*=0.013), which controls melanosome maturation (Cortese et al. 2005). Altogether, the genes with increased expression in the females were significantly enriched for biological processes related to the melanin biosynthetic process (GO:0042438, FE=21.22, FDR=2.54E-04) and pigmentation (GO:0043473, FE=5.74 FDR=0.003).

We also found melanin genes with lower expression level in females than in males, including a member of the semaphorin (SEMA) gene family with prior associations with melanin-based pigmentation in birds (Poelstra et al. 2015; Aguillon et

al. 2021), *SEMA4D* (LFC=-1.31, adj-*p*=4.37E-09), which promotes melanocyte growth and survival (Soong et al. 2012). Additionally, we found increased expression in the reversibly glycosylated polypeptide homolog, *RAB6A* GEF Complex Partner (*RGP1*, LFC=-0.84, adj-*p*=5.8e-07), found in candidate regions of both flickers (*Colaptes auratus auratus/C.a. cafer*) and warblers (*Setophaga coronata audubonii/S. c. coronata*) correlating with melanin production (Brelsford et al. 2017; Aguillon et al. 2021) and unconventional myosin-Va (*MYO5A*, LFC=-0.89, adj-*p*=0.05), which is related to coat color deposition via melanosome transport in other vertebrates (Christen et al. 2021; Zhang et al. 2021). In addition to the genes known to be involved in carotenoid and melanin-based pigmentation, our WGCNA analysis revealed correlated gene modules in the three tissues associated with sexual dichromatism. For details of the WGCNA findings, please refer to the Supplementary Results.

Additional genes may play a role in carotenoid-based sexual dichromatism

Through our transcriptomic analysis, we found additional genes that may play a role in carotenoid-based sexual dichromatism within northern cardinals. Males had upregulated expression of both follistatin (*FST,* LFC=-1.05, adj-*p*=0.04) and Molybdenum cofactor synthesis protein 2A (*MOCS2*, LFC=-1.1, adj-*p*=0.001) in the feather follicles (Figure 4A), which have increased transcription levels in red morphs of Gouldian finches (*Chloebia gouldiae*) compared to the black morphs (Toomey et al. 2018; Kim et al. 2019). *MOCS2,* which was also differentially expressed in the gut, does not appear to be directly linked to pigmentation, but may be associated with the noncoding region upstream of the gene's location. Fatty acid elongase 7 (*ELOVL7*),

296 which regulates red skin color in the leopard coral grouper (Liu et al. 2025), was
297 upregulated in male feather follicles (LFC=-0.82, adj-*p*=0.02; Figure 4A). *ELOVL7* may
298 have a role in carotenoid coloration in birds as the *ELOVL* gene family are implicated in
299 lipid deposition in chickens (Wang et al. 2022), and another gene in the same family,
300 *ELOVL6*, was enriched in male red-backed fairywrens with carotenoid-based coloration
301 (Khalil et al. 2023). Gene ontology analysis of the genes upregulated in the male feather
302 follicles found an overall enrichment for the primary metabolic biological process
303 (GO:0044238, functional enrichment (FE)=1.45, FDR=0.01), suggesting metabolic
304 differences in the feather follicle between the sexes.

305 In the liver, the gene with the greatest magnitude of differential expression was
306 Stearoyl-CoA desaturase (*SCD*, LFC=-3.76, adj-*p*=0.004), which was upregulated in the
307 males. *SCD* is a key regulator in unsaturated fatty acid metabolism and biosynthesis
308 (Flowers and Ntambi 2008; Paton and Ntambi 2009). As unsaturated fatty acids can
309 facilitate the uptake of carotenoids into chylomicrons (Guo et al. 2024), there may be a
310 link between increased *SCD* activity and more efficient carotenoid uptake in males.
311 However, we also found the genes *FST* (LFC=-1.92, adj-*p*=0.01) and *SEMA4D* (LFC=-
312 1.02, adj-*p*=0.007) upregulated in the livers of males. GO analysis of the DEGs
313 upregulated in the male livers did not reveal any statistically significant functional
314 enrichment for the DEGs in this tissue.

315 In the gut, we also found increased transcription in the gene *TTC33* (LFC=-1.08,
316 adj-*p*=0.004), which does not have a known correlation with carotenoid pigmentation but
317 is located within five kilobases of *TTC39B* in the cardinal genome. This region in the
318 northern cardinal maps to the Z chromosome of the *Serinus canaria* genome, consistent

with other species. While investigating for functional enrichment, we found that the genes upregulated in the males were enriched for the biological processes of ribosomal small subunit biogenesis (GO:0042274, FE=8.48, FDR=6.09E-04), rRNA processing (GO:0006364, FE=5.65, FDR=0.002), and DNA repair (GO:0006281, FE=3.20, FDR=0.02). We consulted a previously published list of pigmentation-related genes and their associated PANTHER overrepresentation terms (Baxter et al. 2019) and did not find any of these biological processes listed. Therefore, it is unclear what role these processes may play in pigmentation.

Potential hormonal regulation of sexual dichromatism in the northern cardinal

Our transcriptome analysis provides insights into potential candidate genes related to localized hormonal control of coloration in northern cardinals. We found differential expression in two genes, both located on the Z chromosome, that may serve a role related to the hormonal regulation of sexual dichromatism. 17β-Hydroxysteroid dehydrogenase type IV (*HSD17B4)* was upregulated in males in all the three tissues, with the strongest effect in feather follicles (LFC=-1.11, adj-*p*=9E-13; Figures 4 & S7). *HSD17B4* encodes for an alcohol oxidoreductase that plays a role in many processes including fatty acid β-oxidation, bile acid biosynthesis, sterol transport, and the metabolism of sex steroids (Baes et al. 2000; Breitling et al. 2001; Zhang et al. 2017). Specifically, *HSD17B4* inactivates androgens and estrogens by converting their 17β-hydroxysteroid forms into less active 17-keto forms (Adamski et al. 1995). It therefore likely plays a key role in reducing localized sex steroid receptor signaling activity and hence the associated downstream effects. Another potential regulator is zinc finger

protein 131 (*ZNF131*), which was highly expressed in the feather follicles of males but not females (LFC=-1.45, adj-p=4.1E-8; Figures 4 & S8). *ZNF131* is a repressor of estrogen receptor α (ERα) and negatively regulates estrogen receptor-mediated signaling by interrupting ERα binding to estrogen response elements (EREs) (Han et al. 2008; Oh and Chung 2012).

Discussion

Overall, we found many transcriptomic and carotenoid concentration differences between male and female cardinals. Our observation of higher concentrations of plasma ketocarotenoids in the males compared to the females despite similar concentrations of dietary carotenoids, canary xanthophylls, and non-ketocarotenoids between the sexes suggests that at least some of the differences in production of carotenoid pigments occurs before pigments reach the feather follicle or bill. Similarly, in zebra finches, which lack carotenoids in their plumage, males have redder bills and circulate higher concentrations of carotenoids in their plasma compared to females (McGraw, Gregory, et al. 2003). Additionally, in wild-caught white-winged crossbills (*Loxia leucoptera*), which have carotenoid-based plumage dichromatism like cardinals but without ketocarotenoids in their bills, females and males had no significant difference in plasma lutein/zeaxanthin concentrations but the males exhibited significantly higher concentrations of circulating ketocarotenoids (Deviche et al. 2008). Since feather follicles had higher concentrations of both canary xanthophylls and ketocarotenoids compared to the plasma, it is likely that carotenoid metabolism is occurring primarily within the feather follicles, but it remains to be determined how carotenoid metabolism is

coordinated among tissues. As we also confirmed that the gene products of northern cardinal homologs of *CYP2J19, TTC39B,* and *BDH1L* are sufficient to convert lutein/zeaxanthin to red ketocarotenoids, these genes should be correspondingly upregulated in males.

Expression of *BDH1L*, *CYP2J19*, and *TTC39B* in both the liver and feather follicles supports our hypothesis that ketocarotenoid metabolism occurs in these two tissues, consistent with our prediction based on our observation that ketocarotenoids occur both in circulation and in feather follicles. The almost 24-fold increase in transcription of *CYP2J19* in the feather follicle compared to the liver in both sexes (Figure 5) suggests that even though some canary xanthophylls and ketocarotenoids are produced in the liver, feather follicles are the major site of ketocarotenoid metabolism. In males, higher *CYP2J19* expression in the liver may contribute to sexual dichromatism by increasing ketocarotenoid production and therefore the level of circulating plasma ketocarotenoids. In addition, upregulation of *TTC39B* in male feather follicles likely contributes to the higher concentration of canary xanthophylls and ketocarotenoids in this tissue. However, since *BDH1L*, *CYP2J19*, and *TTC39B* were also expressed in females, and females had a high overall level of *CYP2J19* expression in feather follicles, the differential expression of *CYP2J19* and *TTC39B* cannot entirely explain observations that the breast feathers of females have a drab coloration with almost no ketocarotenoids.

Our observations of differences in expression of genes that may have roles in carotenoid uptake and transportation likely drive some of the plumage differences observed in sexually dichromatic birds. As carotenoids are hydrophobic molecules

transported along with lipid (Granneman et al. 2017; Harrison 2019), the upregulation of lipid transporters in the male northern cardinals compared to the females indicates that sex-specific carotenoid uptake and transport may influence the number of carotenoids available for deposition in the feathers. Higher expression of *SLC27A6* and *PLIN2* in males in both the feather follicles and gut tissues indicates that the same genes and mechanism may be responsible for increasing carotenoid absorption from the food to the bloodstream and carotenoid transfer from the bloodstream to the feather follicles. Prior work in the red-billed quelea (*Quelea quelea*) established *PLIN* as a candidate carotenoid coloration gene (Walsh et al. 2012) but did not find evidence of sexual dichromatism in this gene. *PLIN* was later found differentially expressed between red and buff feather patches in male golden pheasants (*Chrysolophus pictus*) (Gao et al. 2016), but this study did not involve female birds for a complete comparison. *CD36,* which had increased expression in the feather follicle of males, regulates red skin color in leopard coral grouper (*Plectropomus leopardus*) (Jin et al. 2024) and is associated with skin yellowness in chickens (Zhao et al. 2023), suggesting its role in carotenoid transport and coloration in vertebrates. Collectively, the increased expression of these lipid transport genes suggests that enhanced carotenoid absorption and deposition among male northern cardinals may contribute to sexual dichromatism.

Despite the observed differences in genes related to carotenoid uptake, modification, and transport, the large increase in *BCO2* expression in female northern cardinals suggests that this is a gene of major effect in determining the level of carotenoids in feathers. The carotenoid-cleavage activity of *BCO2* is important for mediating the accumulation of carotenoids in tissues (Eriksson et al. 2008; Amengual et

al. 2011; Amengual et al. 2013; Ahi et al. 2020) and contributes to differential carotenoid breakdown and therefore sexual dichromatism in the breast feathers of *mosaic* canaries and European serins (*Serinus serinus*) (Gazda, et al. 2020a). The study in European serins found that *BCO2* is a gene of major effect in modulating carotenoid-based sexual dichromatism in a wild bird population (Gazda, et al. 2020a). Given that female cardinals expressed *BDH1L*, *CYP2J19*, and *TTC39B* at similar levels to the males in most sampled tissues and, indeed, have red feathers in some plumage patches such as the crest, tail, and flight feathers (Figure 1), this physiology must be fully functional and active in ketocarotenoid production in both sexes. Females may compensate for ketocarotenoid production by highly upregulating *BCO2* to cleave carotenoids in the feather follicles of unornamented body regions, leading to the loss of ketocarotenoid coloration. However, the cleavage of carotenoids is not the only mechanism responsible for creating sexual dichromatism in the northern cardinal.

The sexual dichromatism of northern cardinals is not only due to a difference in carotenoid pigmentation, but also melanin-based coloration between the two sexes. While we did not sample feathers in the melanin-dominated black (male) or gray (female) masks of the cardinals, males and females differ in melanin-based coloration in the body plumage we sampled. Females retain melanin-based brownish plumage that is like male juvenile plumage whereas males have reduced melanin in their body feathers to likely enhance the chroma and brightness of ornamental red coloration (Price-Waldman et al. 2025). We found differential expression of many of the genes that are well-known to play a role in melanin-based plumage coloration (McNamara et al. 2021;

Wakamatsu and Ito 2021), demonstrating potential molecular mechanisms underlying melanin-based sexual dichromatism.

The transcriptomic differences between sexes revealed other candidate genes potentially related to sexual dichromatism. One of the most interesting observations of a non-target gene was the upregulation of *FST* in the males. *FST* is indirectly linked through genome-wide association studies to coloration differences in other bird species that do not have red plumage such as the pied flycatcher (*Ficedula hypoleuca*) (Lehtonen et al. 2012) as well as those that utilize carotenoid-based pigmentation such as the golden-winged (*Vermivora chrysoptera*) and blue-winged (*V. cyanoptera*) warblers (Toews et al. 2016). *FST* acts as an antagonist on genes in the *TGF-β* superfamily, which may control melanogenesis (Sharov et al. 2005; McDowall et al. 2008; Moustakas 2008). However, *FST* is also involved in feather morphogenesis (Ohyama et al. 2001; Widelitz et al. 2003) so there may be a structural difference in the feathers between the sexes that affects chroma or brightness, such as barb or barbule shape and density (Igic et al. 2018). If *FST* contributes to structural coloration, it may contribute to increased brilliance of the feathers of male cardinals. As plumage color intensity in northern cardinals is correlated with body condition and positively selected for by females (Jawor 2003; Jawor et al. 2004; Jawor and Breitwisch 2004), sexual selection may have favored the evolution of an additional pathway to maximize plumage intensity.

Our investigation into potential hormonal regulators of northern cardinal dichromatism yielded two candidates. As *HSD17B4* was upregulated in males and downregulated in females, upregulation of this gene suggests greater interconversion of estrogens/androgens which may correspond with increased conversion of estradiol into

454 less active estrone in males. If *BCO2* is upregulated by estrogens in northern cardinals,
455 the lower level of estradiol should therefore reduce *BCO2* expression in males.
456 However, while the higher expression of *HSD17B4* was associated with masculinizing
457 male zebra finch brains, there was not a clear difference in the activity of the encoded
458 enzyme between the sexes (London et al. 2010), so the relationship between *HSD17B4*
459 expression and sex hormone interconversion remains to be resolved. The higher
460 expression of *ZNF131* in male feather follicles may inhibit estrogen signaling and
461 potentially suppress *BCO2* expression. Although the sexual dichromatism in northern
462 cardinals is likely driven by estrogen, androgen-mediated signaling may still contribute,
463 given the upregulation of genes related to carotenoid uptake and metabolism in males,
464 such as *CYP2J19*. Prior work in northern cardinals reported the presence of
465 transcription factor binding motifs associated with androgen signaling upstream of
466 *CYP2J19* (Sin et al. 2020). An androgen-mediated mechanism would be like that found
467 in red-backed fairywrens where testosterone implantation led to the upregulation of
468 *CYP2J19* and development of red plumage in otherwise unornamented males (Khalil et
469 al. 2023). However, fully exploring the links between the genes mentioned here, steroid
470 hormones, and their effects on sexual dichromatism is beyond the scope of this work
471 and remains an area ripe for investigation.

472 Our findings provide further context to and may provide important insight into the
473 debates surrounding the evolutionary origins of sexual dichromatism. Comparative
474 studies in various clades of birds have shown that evolution of sexual dichromatism was
475 often driven by changes in female but not male coloration (Björklund 1991; Irwin 1994;
476 Burns 1998; Hofmann et al. 2008; Johnson et al. 2013; Dale et al. 2015; Simpson et al.

2015; Maia et al. 2016; Price et al. 2024). Therefore, sexual selection may have a less important role in shaping dichromatism than natural selection that drives the loss of female ornamentation (Martin and Badyaev 1996). However, evidence from Tyrannida passerine birds suggests that sexual selection led to rapid divergence in male carotenoid-based coloration rather than any evolution in female plumage (Cooney et al. 2019). Comparative work across Thraupidae and Cardinalidae has indicated that sexual dimorphism in birds occurs via both sexual and natural selection (Shultz and Burns 2017; Porzio and Mota 2025). Our findings also support both evolutionary mechanisms driving sexual dichromatism in northern cardinals. We found that *BCO2* is highly expressed in the feather follicles of females, corresponding with ketocarotenoid breakdown and the loss of red plumage color. This supports natural selection driving the evolution of a molecular mechanism for cryptic coloration in females, as nest site predation correlates with female but not male plumage (Martin and Badyaev 1996). Although females evolved cryptic coloration, they still possess red coloration in their crests, wingtips, and tails, suggesting a yet-unexplored mechanism whereby *BCO2* expression is modulated in these feather patches. In males, upregulation of *CYP2J19* and *TTC39B* in the liver and feather follicle indicates carotenoid breakdown by *BCO2* in females is not the only mechanism contributing to sexual dichromatism. One possible explanation for the differential expression of these carotenoid metabolism genes is that the red plumage in males was driven by sexual selection to become redder in color by elevating the expression level of *TTC39B* and *CYP2J19*. As carotenoid transfer genes were also upregulated in males across sampled tissues, this, along with observations of higher levels of ketocarotenoids in both plasma and feather follicles, likely contributes to

500 the red color of male plumage. Furthermore, genes that are important for melanin-based
501 coloration also play a role in sexual dichromatism. Most melanogenesis genes were
502 expressed at lower levels in male feather follicles compared to females. Thus, males
503 may have evolved reduced melanin-based plumage coloration instead of females
504 evolving increased melanin in the feathers, which could also have resulted from sexual
505 selection for molecular mechanisms that enhance ketocarotenoid plumage coloration in
506 males.

507 These differing selective pressures experienced between male and female birds
508 could lead to the evolution of mechanisms favoring sexual selection that would be
509 counter to natural selection (Coyne et al. 2007). This may ultimately lead to a form of
510 sexual antagonism that would in turn create sex-biased changes in gene expression or
511 other mechanisms of sex-specific regulation (Connallon and Clark 2010). In light of this,
512 the mechanism of *BCO2* upregulation in female birds in several species where males
513 exhibit carotenoid- and ketocarotenoid-based coloration may represent a form of
514 compensation for sexually antagonistic selection. Under sexual conflict driven by sexual
515 antagonism, we would expect to see alleles that favor selection in one sex in turn being
516 detrimental to the other sex and thus subjected to sex-specific regulation (Coyne et al.
517 2007). Such a scenario may contribute to the differential expression in *TTC39B,* located
518 on the Z chromosome, in the feather follicle between the sexes (Figure 5). Sexually
519 antagonistic loci that are detrimental to females are theorized to occur more often on the
520 Z chromosome in birds (Mank and Ellegren 2009; Naurin et al. 2012; Huang and
521 Rabosky 2015). In our findings, the upregulation of *TTC39B* in male feather follicles
522 matches this pattern, as there is incomplete and reduced dosage compensation in birds

(Ellegren et al. 2007; Arnold et al. 2008), which would naturally result in increased expression of Z chromosome genes in males.

In northern cardinals, sexual selection is promoting mutations that enhance the accumulation of red ketocarotenoids in males, which may account for genomic changes such as the large insertion containing many transcription factor binding sites located upstream of *CYP2J19* (Sin et al. 2020), which is an autosomal gene. As, over time, some of these mutations increased *CYP2J19* expression and thus drove maladaptive, increased ketocarotenoid accumulation in females, females evolved an entirely separate mechanism (*BCO2* upregulation) to modify color. This upregulation of *BCO2* in adult females matches theory on sexual antagonism where female-biased genes are upregulated in mature females (Mank and Ellegren 2009). However, this hypothesis also suggests that female-biased genes would be downregulated in males, but from our experimental design it is not possible to determine if *BCO2* is actively downregulated in mature males or if little to no transcription of *BCO2* occurs in both immature and mature males. Despite this and given the fact that red plumage is sexually selected for in males, it is probable that increased expression of *BCO2* and its resulting enzymatic activity is detrimental to mature males and thus is actively downregulated, perhaps by a localized hormonal mechanism.

Another possibility contributing to the scenario in northern cardinals not matching classic sexual antagonism theory is that ketocarotenoid coloration may not be completely detrimental to female cardinals. As assortative mating occurs in both sexes of northern cardinals based on the redness of their plumage (Jawor 2003), it is possible that the antagonistic evolution of red coloration generated another selective method

546 whereby females indicate their quality to males despite contrary selection toward cryptic
547 plumage. Prior work has determined that both bill and underwing redness in females
548 correlate with body size and condition (Jawor et al. 2004), further adding to the
549 evidence for a delicate interplay between natural and sexual selection experienced by
550 northern cardinals. Our findings, in this context, provide an intriguing look into the
551 mechanisms promoting, creating, and controlling sexual dichromatism in birds and lead
552 to many exciting avenues of future exploration and investigation from comparative,
553 endocrinological, and genomic standpoints.
554
555 **Conclusion**

556 By assessing differential expression of genes between male and female
557 northern cardinals in gut, liver, and feather follicle tissues, we determined that sexual
558 dichromatism is largely attributed to the action of a few genes, in particular *BCO2* in
559 the developing feather. Carotenoid breakdown is the major action leading to a loss of
560 red plumage color in females, who also have a corresponding increase in expression
561 of melanogenesis-related genes. The more saturated and extensive red coloration in
562 males is related to enhanced carotenoid uptake and metabolism. Our results indicate
563 that differences in the absorption, metabolism, and transportation of carotenoids
564 between males and females sets the stage for sexual dichromatism in northern
565 cardinals. Importantly, the breakdown of carotenoids at the site of deposition in
566 females results in their much drabber appearance compared to males. Establishing
567 the genetic and molecular basis of the development of sex-specific coloration provides
568 a platform for further studies into the evolution of sexual dichromatism. In the northern

cardinal, a combination of selective forces likely drive and maintain sexual dichromatism. These conflicting, sexually antagonistic evolutionary pressures likely led to both the high transcription of *CYP2J19* in feather follicles regardless of sex and the resulting compensatory mechanism of *BCO2* cleaving carotenoids in female plumage. Further analysis, including sampling from different feather regions and leveraging epigenomics, could provide insight into the intriguing basis of sexual dichromatism in northern cardinals, especially in determining the genetic control of increased ketocarotenoid metabolism and how and to what degree noncoding regions and localized regulatory factors contribute to sexual dichromatism in this species. This work adds to the rich and rapidly expanding body of literature on coloration genetics as well as opens the floor to new questions and explorations into the mechanisms generating some of the incredible biodiversity of the natural world.

Materials & Methods

Sample Collection and Study Design

Sample collection and study design follows a prior experiment; for full details see Patton et al. (2026). Briefly, we caught 11 female and 14 male cardinals using mist nets and Potter traps in Lee County, Alabama, USA from August 14-30, 2023 (see Supplementary Table S3 for specific dates). This collection period falls after the breeding season of northern cardinals but during definitive prebasic molt (Pyle 1997), which is similar in both timing, duration, and mass of feathers replaced in males and females. Blood samples were taken at capture via puncture of the brachial vein using a 28-gauge sterile needle. Birds were weighed, measured for wing and tail length, and assigned numeric values for molt score following Ginn and Melville (1983), where old feathers were assigned a 0, growing feathers assigned 1–4 for increasing stages of development, and fully-grown new feathers given a 5. Average bill hue, average bill saturation, and average bill brightness were assessed using reflectance spectrophotometry in the HSB system. All birds were sampled while in early stages of replacing body plumage estimated as regrowing 4-34% of their plumage at the time of sampling, with the remainder of plumage yet to be replaced. Following euthanasia, follicles of similar developmental stage (about 2 days after first emergence) were individually plucked from the breasts of the carcasses with tweezers, transferred to cryotubes (10-12 follicles per tube), and frozen at -80ºC until used for either carotenoid or RNA analysis to maintain a consistent growth stage and region for comparison in our analyses. We also dissected and flash-froze liver and gut tissue from each individual for RNA analysis.

Carotenoid Analysis

To quantify and characterize carotenoids in feather follicles and blood plasma, we used High-Performance Liquid Chromatography (HPLC), also following methods completely outlined in Patton et al. (2026). In brief, depending on the available sample amount, we extracted either 10µL, 5µL, or 3µL of plasma and added it to 250µL of 100% ethanol. Feather follicles were weighed to the nearest 0.0001g using an analytical balance and homogenized using 500 µL of 0.9% NaCl in water and 0.1g of silica beads in a Beadbug Homogenizer (Benchmark Scientific Inc.) at 4 kHz for 60 seconds. Pilot analysis of feather follicles determined that fatty acid ester removal via saponification was unnecessary. For each tissue type we then vortexed the solution for 5 seconds, added 250 µL of 1:1 Hexane: Methyl tert-butyl ether (MTBE), vortexed again, and then centrifuged for 3 minutes at 10,000 RPM. The prior steps were repeated until the supernatant became transparent and then we capped the vials under nitrogen gas and stored them in a -80ºC freezer. The samples were dissolved in 120 µL of 44:44:12 mobile phase (acetonitrile: methanol: dichloromethane). 100 µL of the sample was injected into an Agilent 1200 Series HPLC with a C30 carotenoid column (5.0 µm, 4.6 × 250 mm, YMC, CT99S05-2546WT) following methods from Koch et al. (2024). Specific carotenoid identities were determined by column retention time and comparison to previously established standards (details in Koch et al. 2025). Carotenoids were quantified by comparison to external standard curves as described in Koch et al. (2025). Non-ketocarotenoids were measured at 445 nm, while ketocarotenoids were measured at 480 nm wavelength using a UV–Vis photodiode array detector. Tissue concentrations of the specific carotenoids were calculated by dividing the determined carotenoid mass

by the mass or volume of the sample. We used R (R Core Team 2023) for all statistical analyses and data plotting. We used Wilcoxon rank-sum (also known as Mann-Whitney U) nonparametric statistics to compare accumulation between male and female birds.

Functional Testing

We performed functional tests following Koch et al. (2025) and Toomey et al. (2022). We determined the coding sequences of the northern cardinal homologs of *CYP2J19, BDH1L*, and *TTC39B* by searching the reference genome (GenBank accession GCA_014549065.1) via BLAST (Sayers et al. 2025) with a query of the known functional house finch homologs (sequences in Koch et al. 2025). We then extracted ~50kb of the reference sequence centered on the BLAST hit and used AUGUSTUS (Hoff and Stanke 2013) to predict genes within this region. We validated these gene predictions by alignment of raw RNA sequencing reads and comparison to the *de novo* assembled transcripts (below). We then translated the validated transcript sequences to amino acid sequences (Supplementary Table S2) and synthesized human codon optimized DNA fragments through a commercial service (Twist Biosciences, San Francisco, CA). We cloned these fragments into the first position of the eukaryotic expression vector *pCAG-[first position]-2A-GFP* or *pCAG-[first position]-2A-dsRed*. This vector produces a single transcript containing the candidate gene and the fluorescent tag (GFP or dsRed) that results in the stoichiometric translation of two peptides through a ribosomal skipping event. Thus, the fluorescent protein is indicative of candidate gene expression. We co-transfected the three constructs containing *CYP2J19, BDH1L,* or *TTC39*B into HEK293 (CRL-1573, ATCC) using polyethylenimine (PEI). The HEK293 cells were cultured with the media formulation and protocols recommended by

American Type Culture Collection (ATCC). As a control, we separately transfected HEK293 cultures with constructs containing fluorescent protein sequences in both positions of the construct (i.e. *pCAG-dsRed-2A-GFP*). We incubated the cells overnight and confirmed expression by visualizing fluorescence protein with an epifluorescence microscope. We then supplemented the culture media with 1 µg of either lutein (Floraglo, 5011868022, DSM Inc.) or zeaxanthin (Optisharp, 5003563004, DSM Inc.) per 1mL solubilized with 0.035% (w:v) polysorbate 40 (Acros Organics, AC334142500). For additional details on carotenoid purification and preparation please refer to Toomey et al. (2025). We then incubated the experimental and control cultures overnight, harvested the cells by scraping the culture plates, washed the cells twice with phosphate-buffered saline, then extracted and analyzed the carotenoid content of the cells by HPLC following the methods described for liver and gut tissue above.

RNA extraction, library preparation, and sequencing

We extracted RNA from our tissue samples using the Trizol reagent following the manufacturer's suggested protocols and homogenizing on a beadmill (15596026, Invitrogen). Contaminating DNA was removed by treating the samples with Turbo DNase reagent (AM2238, Invitrogen) and the treated RNA recovered by chloroform extraction followed by sodium acetate precipitation. The RNA was then dissolved in 35 µL of RNAse-free water and quantified using a Qubit fluorometer (Thermo Fisher). Library preparation and sequencing was completed by the Oklahoma Medical Research Foundation's Clinical Genomics Center. Briefly, 250 ng of RNA from each tissue type (feather follicle/liver/gut) was prepared for poly-A selected mRNA sequencing using the

672 xGen RNA Library Preparation Kit from Integrated DNA Technologies (Coralville, Iowa,
673 USA). Samples were sequenced on the NovaSeq PE150.

674 *Genome annotation*

675 For annotation of the existing Northern cardinal genome (Sin et al. 2020), we
676 built a *de novo* transcriptome using TRINITY v 2.14.0 (Grabherr et al. 2011). We
677 combined RNA-seq data from a cardinal blood sample from the NCBI SRA
678 (SRX7523501), and sequencing data from a single male and female individual feather
679 follicle, liver, and gut tissue. We used the default settings within TRINITY, including the
680 recommended quality trimming using TRIMMOMATIC (Bolger et al. 2014) with the
681 following parameters: "ILLUMINACLIP:TruSeq3-PE.fa:2:30:10 SLIDINGWINDOW:4:5
682 LEADING:5 TRAILING:5 MINLEN:25". Following transcript assembly, we used the
683 transcriptome as additional evidence for performing *ab initio* gene prediction using
684 MAKER v 3.01.03 (Cantarel et al. 2008; Holt and Yandell 2011), the AUGUSTUS
685 chicken database (Stanke et al. 2006), and the RepBase for aves (Bao et al. 2015). We
686 performed annotation finalization and homology prediction using GeMoMa (Keilwagen
687 et al. 2019) and reference annotations from other passerines including the house finch
688 *Haemorhous mexicanus* (GenBank accession GCA_027477595.1), common canary
689 *Serinus canaria* (GenBank accession GCA_022539315.2), great tit *Parus major*
690 (GenBank accession GCA_001522545.3), and zebra finch *Taeniopygia guttata*
691 (GenBank accession GCA_003957565.4). We performed genome re-annotation and
692 functional annotation using eggNOG (Huerta-Cepas et al. 2019).

Transcriptomic data analysis

We preprocessed the RNA-seq data using Fastp v0.23.2 (Chen et al. 2018) to remove low-quality bases, adapters, and erroneous polyG tails to correct for two-color sequencing bias in the case of short read inserts, and the first 10 bases of read 2 as suggested by the best practices for the xGen RNA library kit. For transcript-based gene expression quantification, we utilized the program RSEM (Li and Dewey 2011). For initial alignment to the reference genome, we used STAR v2.7.9a (Dobin et al. 2013) with modified settings --outFilterType BySJout --outFilterMultimapNmax 20 --alignSJoverhangMin 8 --alignSJDBoverhangMin 1 --outFilterMismatchNmax 999 --outFilterMismatchNoverReadLmax 0.6 --alignIntronMin 20 --alignIntronMax 30000 --alignMatesGapMax 1000000. For secondary alignment, we used the same settings as before but under --quantMode TranscriptomeSAM and using --sjdbFileChrStartEnd with the SJ files generated from the prior alignment. We then passed the output files to rsem-calculate-expression specifying paired-end alignments to calculate expression prior to creating a gene count matrix using rsem-generate-data-matrix.

We read the raw gene counts from all three runs into DESeq2 (Love et al. 2014) using R (R Core Team 2021) and removed genes with no counts across all individuals before checking for library effects using PCA. After confirming the absence of library effects, we collapsed the reads from each library into a single dataset. For tissue-specific analysis, we separated the data by tissue type (feather follicle, gut, and liver) and carried out additional filtration of genes with no counts in the respective tissue. Following that, we used a final filter from edgeR (Robinson et al. 2010) “filterByExpr()” to remove uninformative genes from each dataset. We performed additional

716 independent hypothesis weighting within DESeq2 to adjust for the covariate of the sum
717 of read counts per gene across all samples and control for false discovery rate
718 (Ignatiadis et al. 2016). We then compared expression levels between the males and
719 females to determine differential expression related to sex. When visualizing single
720 genes across tissues, we extracted transcripts per million (TPM) data from RSEM
721 output files and plotted the data using R.

722 For weighted gene co-expression analysis (WGCNA), we used the WGCNA
723 package in R (Langfelder and Horvath 2008). Following best practices for this analysis,
724 we used a variance stabilizing transformation on our expression data for each tissue
725 type. We removed outlier samples based on visualizing the cluster dendrogram of
726 samples for each analysis. When calculating our soft threshold for adjacency analysis,
727 we utilized the built-in method for power estimation under default settings, which relies
728 on a mean connectivity threshold of 0.85. For the feather follicle, gut, and liver datasets
729 we used the recommended powers of 6, 9, and 10, respectively. For each tissue type,
730 we set a minimum size per module of 30 genes and used a threshold of 0.25 to merge
731 highly correlated gene modules. For finding correlations between gene modules and
732 phenotypes of interest, we used numerical factors for sex (i.e. females=1, males=2). We
733 also incorporated measurements of wing length, tail length, weight, molt score, average
734 bill hue/saturation/brightness while molting, and plasma/follicle xanthophyll,
735 ketocarotenoid, and non-ketocarotenoid carotenoid measurements from high-
736 performance liquid chromatography (HPLC). As there was missing information in a few
737 individuals for the wing/tail/weight measurements, we imputed these values using the
738 imputePCA() function from the R package missMDA (Josse and Husson 2016) and then

calculated a body condition ratio using the wing length and weight. For modules with a significant ($p<0.05$) correlation with a phenotypic variable, we confirmed that the genes within the module also had a significant correlation between their calculated significance and module membership as well as a significant difference in average eigengene expression between the phenotypes (Welch t-test, $p<0.05$). We then investigated the gene ontology (GO) enrichment of these modules across biological processes (BP) using the PANTHER database for *Gallus gallus* (Ashburner et al. 2000; Thomas et al. 2022; The Gene Ontology Consortium et al. 2023). We used the Fisher test with correction for false discovery rate (FDR) to assess significance.

Supplementary materials

Supplementary materials includes 8 figures and 6 tables and can be found with this article online.

Acknowledgements

The computations were performed using research computing facilities offered by Information Technology Services, the University of Hong Kong.

Ethics Statement

All research was conducted under approved IACUC permit #2023-5246 at Auburn University, along with compliance of Alabama state permit #2023124515668680 and United States federal permit #MPBER1562352.

Funding

This project was supported by the Seed Fund for Basic Research (the University of Hong Kong) granted to S.Y.W.S; funding from the National Science Foundation (NSF) (IOS 2037739), the College of Engineering and Natural Sciences at the University of Tulsa, and the Tulsa Undergraduate Research Challenge to M.B.T.; NSF funding (IOS 2037741) to G.E.H.; NSF funding (IOS-2037735 and IOS-2224556) to Y.Z.

Data Availability

Raw count data for this project are available from the HKU DataHub, DOI: 10.25442/hku.30828212; R scripts for the project can be obtained upon request.

Author contributions

Conceptualization: SYWS, GEH, MBT, YZ; formal Analysis: MJW; funding acquisition: SYWS, MBT, GEH, YZ; investigation: SP, ES, REK; methodology: SYWS, GEH, MBT, MJW, YZ; resources: SYWS, GEH, MBT, YZ; supervision: SYWS; visualization: MJW; writing—original draft: MJW, SYWS; writing—review & editing: MJW, SYWS, GEH, MBT, YZ, REK.

Conflicts of Interest

The authors declare no conflicts of interest.

References

Adamski J et al. 1995. Molecular cloning of a novel widely expressed human 80 kDa 17 beta-hydroxysteroid dehydrogenase IV. *Biochem J* 311 (Pt 2):437–443.

Adelmann CH et al. 2020. MFSD12 mediates the import of cysteine into melanosomes and lysosomes. *Nature* 588:699–704.

Aguillon SM, Walsh J, Lovette IJ. 2021. Extensive hybridization reveals multiple coloration genes underlying a complex plumage phenotype. *Proc. R. Soc. B.* 288:20201805.

Ahi EP et al. 2020. Comparative transcriptomics reveals candidate carotenoid color genes in an East African cichlid fish. *BMC Genomics* 21:54.

Alonso-Alvarez C, Andrade P, Cantarero A, Morales J, Carneiro M. 2022. Relocation to avoid costs: A hypothesis on red carotenoid-based signals based on recent *CYP2J19* gene expression data. *BioEssays* 44:2200037.

Amengual J et al. 2011. A mitochondrial enzyme degrades carotenoids and protects against oxidative stress. *FASEB J* 25:948–959.

Amengual J et al. 2013. Two carotenoid oxygenases contribute to mammalian provitamin A metabolism. *J Biol Chem* 288:34081–34096.

Arnold AP, Itoh Y, Melamed E. 2008. A bird's-eye view of sex chromosome dosage compensation. *Annu Rev Genomics Hum Genet* 9:109–127.

Ashburner M et al. 2000. Gene Ontology: tool for the unification of biology. *Nat Genet* 25:25–29.

Badyaev AV, Hill GE. 2000. Evolution of sexual dichromatism: contribution of carotenoid- versus melanin-based coloration. *Biological Journal of the Linnean Society* 69:153–172.

Baes M et al. 2000. Inactivation of the peroxisomal multifunctional protein-2 in mice impedes the degradation of not only 2-methyl-branched fatty acids and bile acid intermediates but also of very long chain fatty acids. *J Biol Chem* 275:16329–16336.

Baiz MD, Wood AW, Brelsford A, Lovette IJ, Toews DPL. 2021. Pigmentation Genes Show Evidence of Repeated Divergence and Multiple Bouts of Introgression in Setophaga Warblers. *Current Biology* 31:643-649.e3.

Bao W, Kojima KK, Kohany O. 2015. Repbase Update, a database of repetitive elements in eukaryotic genomes. *Mobile DNA* 6:11.

Baxter LL, Watkins-Chow DE, Pavan WJ, Loftus SK. 2019. A curated gene list for expanding the horizons of pigmentation biology. *Pigment Cell Melanoma Res* 32:348–358.

Björklund M. 1991. Coming of age in fringillid birds: heterochrony in the ontogeny of secondary sexual characters. *J of Evolutionary Biology* 4:83–92.

Bolger AM, Lohse M, Usadel B. 2014. Trimmomatic: a flexible trimmer for Illumina sequence data. *Bioinformatics* 30:2114–2120.

Bourgeois YXC, Bertrand JAM, Thébaud C, Milá B. 2012. Investigating the Role of the Melanocortin-1 Receptor Gene in an Extreme Case of Microgeographical Variation in the Pattern of Melanin-Based Plumage Pigmentation.Lalueza-Fox C, editor. *PLoS ONE* 7:e50906.

Breitling R, Marijanović Z, Perović D, Adamski J. 2001. Evolution of 17β-HSD type 4, a multifunctional protein of β-oxidation. *Molecular and Cellular Endocrinology* 171:205–210.

Brelsford A, Toews DPL, Irwin DE. 2017. Admixture mapping in a hybrid zone reveals loci associated with avian feather coloration. *Proc. R. Soc. B.* 284:20171106.

Burns KJ. 1998. A phylogenetic perspective on the evolution of sexual dichromatism in tanagers (thraupidae): the role of female versus male plumage. *Evolution* 52:1219–1224.

Cantarel BL et al. 2008. MAKER: an easy-to-use annotation pipeline designed for emerging model organism genomes. *Genome Res* 18:188–196.

Chen H et al. 2021. Analysis of recently duplicated *TYRP1* genes and their effect on the formation of black patches in Oujiang-color common carp (*Cyprinus carpio* var. *color*). *Animal Genetics* 52:451–460.

Chen S, Zhou Y, Chen Y, Gu J. 2018. fastp: an ultra-fast all-in-one FASTQ preprocessor. *Bioinformatics* 34:i884–i890.

Christen M, de le Roi M, Jagannathan V, Becker K, Leeb T. 2021. MYO5A Frameshift Variant in a Miniature Dachshund with Coat Color Dilution and Neurological Defects Resembling Human Griscelli Syndrome Type 1. *Genes (Basel)* 12:1479.

Connallon T, Clark AG. 2010. Sex linkage, sex-specific selection, and the role of recombination in the evolution of sexually dimorphic gene expression: sex linkage and sexual dimorphism. *Evolution* 64:3417–3442.

Cooney CR et al. 2019. Sexual selection predicts the rate and direction of colour divergence in a large avian radiation. *Nat Commun* 10:1773.

Cortese K et al. 2005. The ocular albinism type 1 (OA1) gene controls melanosome

maturation and size. *Invest Ophthalmol Vis Sci* 46:4358–4364.

Coyne JA, Kay EH, Pruett-Jones S. 2007. The Genetic Basis of Sexual Dichromatism in Birds. *Evolution* 62:214–219.

Dale J, Dey CJ, Delhey K, Kempenaers B, Valcu M. 2015. The effects of life history and sexual selection on male and female plumage colouration. *Nature* 527:367–370.

Dela Seña C et al. 2016. Substrate Specificity of Purified Recombinant Chicken β-Carotene 9′,10′-Oxygenase (BCO2). *Journal of Biological Chemistry* 291:14609–14619.

Delhey K, Peters A. 2017. The effect of colour-producing mechanisms on plumage sexual dichromatism in passerines and parrots.Rezende E, editor. *Functional Ecology* 31:903–914.

Deviche P, McGraw KJ, Underwood J. 2008. Season-, sex-, and age-specific accumulation of plasma carotenoid pigments in free-ranging white-winged crossbills *Loxia leucoptera*. *Journal of Avian Biology* 39:283–292.

Dobin A et al. 2013. STAR: ultrafast universal RNA-seq aligner. *Bioinformatics* 29:15–21.

Ellegren H et al. 2007. Faced with inequality: chicken do not have a general dosage compensation of sex-linked genes. *BMC Biol* 5:40.

Enbody ED et al. 2021. A multispecies BCO2 beak color polymorphism in the Darwin's finch radiation. *Curr Biol* 31:5597-5604.e7.

Eriksson J et al. 2008. Identification of the yellow skin gene reveals a hybrid origin of the domestic chicken. *PLoS Genet* 4:e1000010.

Flowers MT, Ntambi JM. 2008. Role of stearoyl-coenzyme A desaturase in regulating lipid metabolism. *Curr Opin Lipidol* 19:248–256.

Gao G-Q, Song L-S, Tong B, Li G-P. 2016. Expression levels of GSTA2 and APOD genes might be associated with carotenoid coloration in golden pheasant (Chrysolophus pictus) plumage. *Zoological Research* 37:144–150.

Gazda MA et al. 2020a. A genetic mechanism for sexual dichromatism in birds. *Science* 368:1270–1274.

Gazda MA et al. 2020b. Genetic Basis of De Novo Appearance of Carotenoid Ornamentation in Bare Parts of Canaries.Wittkopp P, editor. *Molecular Biology and Evolution* 37:1317–1328.

Ginn, H. B. and Melville, D. S. 1983. Moult in birds. BTO Guide 19. British Trust for Ornithology.

882 Grabherr MG et al. 2011. Full-length transcriptome assembly from RNA-Seq data
883 without a reference genome. *Nat Biotechnol* 29:644–652.

884 Granneman JG et al. 2017. Lipid droplet biology and evolution illuminated by the
885 characterization of a novel perilipin in teleost fish. *eLife* 6:e21771.

886 Guo Z, Liu Y, Luo Y. 2024. Mechanisms of carotenoid intestinal absorption and the
887 regulation of dietary lipids: lipid transporter-mediated transintestinal epithelial
888 pathways. *Critical Reviews in Food Science and Nutrition* 64:1791–1816.

889 Han X et al. 2008. High-throughput cell-based screening reveals a role for ZNF131 as a
890 repressor of ERalpha signaling. *BMC Genomics* 9:476.

891 Harrison EH. 2019. Mechanisms of Transport and Delivery of Vitamin A and
892 Carotenoids to the Retinal Pigment Epithelium. *Mol Nutr Food Res* 63:e1801046.

893 Hill GE, Johnson JD. 2012. The Vitamin A–Redox Hypothesis: A Biochemical Basis for
894 Honest Signaling via Carotenoid Pigmentation. *The American Naturalist*
895 180:E127–E150.

896 Hill GE, McGraw KJ eds. 2006a. Bird Coloration, Volume 1: Mechanisms and
897 Measurements. Harvard University Press.

898 Hill GE, McGraw KJ eds. 2006b. Bird Coloration, Volume 2: Function and Evolution.
899 Harvard University Press.

900 Hoff KJ, Stanke M. 2013. WebAUGUSTUS--a web service for training AUGUSTUS and
901 predicting genes in eukaryotes. *Nucleic Acids Research* 41:W123–W128.

902 Hofmann CM, Cronin TW, Omland KE. 2008. Evolution of sexual dichromatism. 1.
903 Convergent losses of elaborate female coloration in new world orioles (*Icterus*
904 spp.). *Auk* 125:778–789.

905 Holt C, Yandell M. 2011. MAKER2: an annotation pipeline and genome-database
906 management tool for second-generation genome projects. *BMC Bioinformatics*
907 12:491.

908 Hooper DM, Griffith SC, Price TD. 2019. Sex chromosome inversions enforce
909 reproductive isolation across an avian hybrid zone. *Molecular Ecology* 28:1246–
910 1262.

911 Hooper DM et al. 2024. Spread of yellow-bill-color alleles favored by selection in the
912 long-tailed finch hybrid system. *Current Biology*:S0960982224013733.

913 Huang H, Rabosky DL. 2015. Sex-linked genomic variation and its relationship to avian
914 plumage dichromatism and sexual selection. *BMC Evol Biol* 15:199.

915 Hubbard JK, Uy JAC, Hauber ME, Hoekstra HE, Safran RJ. 2010. Vertebrate

pigmentation: from underlying genes to adaptive function. *Trends in Genetics* 26:231–239.

Huerta-Cepas J et al. 2019. eggNOG 5.0: a hierarchical, functionally and phylogenetically annotated orthology resource based on 5090 organisms and 2502 viruses. *Nucleic Acids Research* 47:D309–D314.

Igic B, D'Alba L, Shawkey MD. 2018. Fifty shades of white: how white feather brightness differs among species. *Sci Nat* 105:18.

Ignatiadis N, Klaus B, Zaugg JB, Huber W. 2016. Data-driven hypothesis weighting increases detection power in genome-scale multiple testing. *Nat Methods* 13:577–580.

Irwin RE. 1994. The Evolution of Plumage Dichromatism in the New World Blackbirds: Social Selection on Female Brightness. *The American Naturalist* 144:890–907.

Jawor JM. 2003. Assortative mating by multiple ornaments in northern cardinals (Cardinalis cardinalis). *Behavioral Ecology* 14:515–520.

Jawor JM, Breitwisch R. 2004. Multiple Ornaments in Male Northern Cardinals, *Cardinalis cardinalis* , as Indicators of Condition. *Ethology* 110:113–126.

Jawor JM, Gray N, Beall SM, Breitwisch R. 2004. Multiple ornaments correlate with aspects of condition and behaviour in female northern cardinals, Cardinalis cardinalis. *Animal Behaviour* 67:875–882.

Jin C et al. 2024. Deciphering scavenger receptors reveals key regulators in the intestine that function in carotenoid coloration of leopard coral groupers (Plectropomus leopardus). *International Journal of Biological Macromolecules* 260:129387.

Johnson AE, Jordan Price J, Pruett-Jones S. 2013. Different modes of evolution in males and females generate dichromatism in fairy-wrens (M aluridae). *Ecology and Evolution* 3:3030–3046.

Josse J, Husson F. 2016. missMDA: A Package for Handling Missing Values in Multivariate Data Analysis. *J. Stat. Soft.* 70.

Keilwagen J, Hartung F, Grau J. 2019. GeMoMa: Homology-Based Gene Prediction Utilizing Intron Position Conservation and RNA-seq Data. *Methods Mol Biol* 1962:161–177.

Khalil S et al. 2023. Testosterone Coordinates Gene Expression Across Different Tissues to Produce Carotenoid-Based Red Ornamentation. Parsch J, editor. *Molecular Biology and Evolution* 40:msad056.

Kim K-W et al. 2019. Genetics and evidence for balancing selection of a sex-linked

colour polymorphism in a songbird. *Nat Commun* 10:1852.

Kimball RT, Ligon JD. 1999. Evolution of Avian Plumage Dichromatism from a Proximate Perspective. *The American Naturalist* 154:182–193.

Kirschel ANG et al. 2020. *CYP2J19* mediates carotenoid colour introgression across a natural avian hybrid zone. *Molecular Ecology* 29:4970–4984.

Koch RE et al. 2024. Captivity affects mitochondrial aerobic respiration and carotenoid metabolism in the house finch (*Haemorhous mexicanus*). *Journal of Experimental Biology* 227:jeb246980.

Koch RE et al. 2025. Multiple Pathways to Red Carotenoid Coloration: House Finches (*HAEMORHOUS MEXICANUS*) Do Not Use CYP2J19 to Produce Red Plumage. *Molecular Ecology* 34:e17744.

Langfelder P, Horvath S. 2008. WGCNA: an R package for weighted correlation network analysis. *Bmc Bioinformatics* 9:559.

Lee CM et al. 1999. Review of animal models in carotenoid research. *J Nutr* 129:2271–2277.

Lehtonen PK et al. 2012. Candidate genes for colour and vision exhibit signals of selection across the pied flycatcher (Ficedula hypoleuca) breeding range. *Heredity* 108:431–440.

Li B, Dewey CN. 2011. RSEM: accurate transcript quantification from RNA-Seq data with or without a reference genome. *BMC Bioinformatics* 12:323.

Lin G-W et al. 2025. Molecular insights into region-specific sexual dichromatism: Comparative transcriptome analysis of red cheek pigmentation in zebra finches. *PLoS Genet* 21:e1011693.

Liu R et al. 2021. Choline kinase alpha 2 acts as a protein kinase to promote lipolysis of lipid droplets. *Mol Cell* 81:2722-2735.e9.

Liu X et al. 2023. Cluster-determinant 36 (CD36) mediates intestinal absorption of dietary astaxanthin and affects its secretion. *Food Research International* 173:113328.

Liu Y et al. 2025. DNA Methylation and Transcriptome Profiling Reveal the Role of the Antioxidant Pathway and Lipid Metabolism in Plectropomus leopardus Skin Color Formation. *Antioxidants (Basel)* 14:93.

London SE et al. 2010. Neural expression and post-transcriptional dosage compensation of the steroid metabolic enzyme 17beta-HSD type 4. *BMC Neurosci* 11:47.

Lopes RJ et al. 2016. Genetic Basis for Red Coloration in Birds. *Current Biology* 26:1427–1434.

Love MI, Huber W, Anders S. 2014. Moderated estimation of fold change and dispersion for RNA-seq data with DESeq2. *Genome Biol* 15:550.

Lu B et al. 2024. Genetic Basis and Evolutionary Forces of Sexually Dimorphic Color Variation in a Toad-Headed Agamid Lizard. *Mol Biol Evol* 41:msae054.

Lyons LA, Foe IT, Rah HC, Grahn RA. 2005. Chocolate coated cats: TYRP1 mutations for brown color in domestic cats. *Mamm Genome* 16:356–366.

Maia R, Rubenstein DR, Shawkey MD. 2016. Selection, constraint, and the evolution of coloration in African starlings: selection, constraints and color evolution. *Evolution* 70:1064–1079.

Mank JE, Ellegren H. 2009. Sex-linkage of sexually antagonistic genes is predicted by female, but not male, effects in birds. *Evolution* 63:1464–1472.

Martin TE, Badyaev AV. 1996. Sexual dichromatism in birds: importance of nest predation and nest location for females versus males. *Evolution* 50:2454–2460.

McDowall M, Edwards NM, Jahoda C a. B, Hynd PI. 2008. The role of activins and follistatins in skin and hair follicle development and function. *Cytokine Growth Factor Rev* 19:415–426.

McGraw KJ, Gregory AJ, Parker RS, Adkins-Regan E. 2003. Diet, plasma carotenoids, and sexual coloration in the zebra finch (Taeniopygia guttata). *Auk* 120:400.

McGraw KJ, Hill GE, Parker RS. 2003. Carotenoid Pigments in a Mutant Cardinal: Implications for the Genetic and Enzymatic Control Mechanisms of Carotenoid Metabolism in Birds. *The Condor* 105:587–592.

McGraw KJ, Hill GE, Stradi R, Parker RS. 2001. The influence of carotenoid acquisition and utilization on the maintenance of species-typical plumage pigmentation in male American goldfinches (Carduelis tristis) and northern cardinals (Cardinalis cardinalis). *Physiol Biochem Zool* 74:843–852.

McNamara ME et al. 2021. Decoding the Evolution of Melanin in Vertebrates. *Trends in Ecology & Evolution* 36:430–443.

Melo-Rojas C, Bravo-Matheus PW, Amaht Araoz C, Zapata-Coacalla C. 2023. Identification of polymorphisms in TYRP1, DCT and RAB38 genes and their association with coat color in alpacas. *Front. Anim. Sci.* 4:1236582.

Moustakas A. 2008. TGF-beta targets PAX3 to control melanocyte differentiation. *Dev Cell* 15:797–799.

1019 Mundy NI. 2005. A window on the genetics of evolution: MC1R and plumage colouration
1020 in birds. *Proc Biol Sci* 272:1633–1640.

1021 Mundy NI et al. 2016. Red Carotenoid Coloration in the Zebra Finch Is Controlled by a
1022 Cytochrome P450 Gene Cluster. *Current Biology* 26:1435–1440.

1023 Naurin S, Hasselquist D, Bensch S, Hansson B. 2012. Sex-Biased Gene Expression on
1024 the Avian Z Chromosome: Highly Expressed Genes Show Higher Male-Biased
1025 Expression.Nurminsky DI, editor. *PLoS ONE* 7:e46854.

1026 Nishida Y et al. 2023. Astaxanthin: Past, Present, and Future. *Marine Drugs* 21:514.

1027 Oh Y, Chung KC. 2012. Small ubiquitin-like modifier (SUMO) modification of zinc finger
1028 protein 131 potentiates its negative effect on estrogen signaling. *J Biol Chem*
1029 287:17517–17529.

1030 Ohyama A, Saito F, Ohuchi H, Noji S. 2001. Differential expression of two BMP
1031 antagonists, gremlin and Follistatin, during development of the chick feather bud.
1032 *Mechanisms of Development* 100:331–333.

1033 Paton CM, Ntambi JM. 2009. Biochemical and physiological function of stearoyl-CoA
1034 desaturase. *American Journal of Physiology-Endocrinology and Metabolism*
1035 297:E28–E37.

1036 Patton SM, Koch RE, Zhang Y, Toomey MB, Hill GE. 2026. Captivity negatively affects
1037 production of red carotenoid pigments in Cardinalis cardinalis (Northern cardinal),
1038 *Ornithology* ukag010.

1039 Peer BD, Motz RW. 2014. Observations of a Bilateral Gynandromorph Northern
1040 Cardinal (*Cardinalis cardinalis*). *The Wilson Journal of Ornithology* 126:778–
1041 781.

1042 Perez-Beato O. 2008. Fundamentals of color genetics in canaries: reproduction and
1043 control. Place of publication not identified: Rosedog Pr

1044 Poelstra JW, Vijay N, Hoeppner MP, Wolf JBW. 2015. Transcriptomics of colour
1045 patterning and coloration shifts in crows. *Molecular Ecology* 24:4617–4628.

1046 Porzio NS, Mota PG. 2025. Evidence for the evolution of male and female cardinals'
1047 plumage colouration being affected by both natural and sexual selection. *BMC*
1048 *Ecol Evo* 25:116.

1049 Price JJ, Garcia K, Eaton MD. 2024. Losses of sexual dichromatism involve rapid
1050 changes in female plumage colors to match males in New World
1051 blackbirds.Taylor S, Zelditch M, editors. *Evolution* 78:188–194.

1052 Price-Waldman RM, Ali JR, Shultz AJ, Hogan BG, Stoddard MC. 2025. Hidden white
1053 and black feather layers enhance plumage coloration in tanagers and other

songbirds. *Sci. Adv.* 11:eadw5857.

Pyle, P. (1997). Molt limits in North American passerines. *North American Bird Bander* 22:1.

R Core Team. 2021. R: A language and environment for statistical computing. Available from: https://www.R-project.org/

Ranasinghe RW, Hudon J, Seneviratne SS, Irwin D. Biochemical and Genomic Underpinnings of Carotenoid Colour Variation Across a Hybrid Zone Between South Asian Flameback Woodpeckers. *Mol Ecol.* 2025 Oct;34(19):e70084.

Robinson MD, McCarthy DJ, Smyth GK. 2010. edgeR: a Bioconductor package for differential expression analysis of digital gene expression data. *Bioinformatics* 26:139–140.

Sayers EW et al. 2025. Database resources of the National Center for Biotechnology Information in 2025. *Nucleic Acids Res* 53:D20–D29.

Sharov AA et al. 2005. Bone morphogenetic protein (BMP) signaling controls hair pigmentation by means of cross-talk with the melanocortin receptor-1 pathway. *Proc Natl Acad Sci U S A* 102:93–98.

Shultz AJ, Burns KJ. 2017. The role of sexual and natural selection in shaping patterns of sexual dichromatism in the largest family of songbirds (Aves: Thraupidae). *Evolution* 71:1061–1074.

Simpson RK, Johnson MA, Murphy TG. 2015. Migration and the evolution of sexual dichromatism: evolutionary loss of female coloration with migration among wood-warblers. *Proc Biol Sci* 282:20150375.

Sin SYW, Lu L, Edwards SV. 2020. *De Novo* Assembly of the Northern Cardinal (*Cardinalis cardinalis*) Genome Reveals Candidate Regulatory Regions for Sexually Dichromatic Red Plumage Coloration. *G3 Genes|Genomes|Genetics* 10:3541–3548.

Soong J, Chen Y, Shustef EM, Scott GA. 2012. Sema4D, the ligand for Plexin B1, suppresses c-Met activation and migration and promotes melanocyte survival and growth. *J Invest Dermatol* 132:1230–1238.

Stanke M et al. 2006. AUGUSTUS: ab initio prediction of alternative transcripts. *Nucleic Acids Research* 34:W435–W439.

The Gene Ontology Consortium et al. 2023. The Gene Ontology knowledgebase in 2023.Baryshnikova A, editor. *GENETICS* 224:iyad031.

Thomas PD et al. 2022. PANTHER : Making genome-scale phylogenetics accessible to all. *Protein Science* 31:8–22.

1089 Toews DPL, Hofmeister NR, Taylor SA. 2017. The Evolution and Genetics of
1090 Carotenoid Processing in Animals. *Trends in Genetics* 33:171–182.

1091 Toews DPL et al. 2016. Plumage Genes and Little Else Distinguish the Genomes of
1092 Hybridizing Warblers. *Current Biology* 26:2313–2318.

1093 Tomaszycki ML, Dzubur E. 2013. 17β-Hydroxysteroid dehydrogenase Type IV, a Z-
1094 linked gene, is higher in females than in males in visual and auditory regions of
1095 developing zebra finches. *Brain Research* 1520:95–106.

1096 Toomey MB et al. 2025. Substrates, intermediates, and products of avian
1097 ketocarotenoid metabolism. *Biochimica et Biophysica Acta (BBA) - Molecular and*
1098 *Cell Biology of Lipids* 1870:159654.

1099 Toomey MB et al. 2016. Complementary shifts in photoreceptor spectral tuning unlock
1100 the full adaptive potential of ultraviolet vision in birds. *eLife* 5:e15675.

1101 Toomey MB et al. 2017. High-density lipoprotein receptor SCARB1 is required for
1102 carotenoid coloration in birds. *Proc. Natl. Acad. Sci. U.S.A.* 114:5219–5224.

1103 Toomey MB et al. 2018. A non-coding region near *Follistatin* controls head colour
1104 polymorphism in the Gouldian finch. *Proc. R. Soc. B.* 285:20181788.

1105 Toomey MB et al. 2022. A mechanism for red coloration in vertebrates. *Current Biology*
1106 32:4201-4214.e12.

1107 Twyman H, Prager M, Mundy NI, Andersson S. 2018. Expression of a
1108 carotenoid-modifying gene and evolution of red coloration in weaverbirds
1109 (Ploceidae). *Molecular Ecology* 27:449–458.

1110 Wakamatsu K, Ito S. 2021. Melanins in Vertebrates. In: Hashimoto H, Goda M,
1111 Futahashi R, Kelsh R, Akiyama T, editors. Pigments, Pigment Cells and Pigment
1112 Patterns. Singapore: Springer Singapore. p. 45–89.

1113 Walsh N, Dale J, McGraw KJ, Pointer MA, Mundy NI. 2012. Candidate genes for
1114 carotenoid coloration in vertebrates and their expression profiles in the
1115 carotenoid-containing plumage and bill of a wild bird. *Proc. R. Soc. B.* 279:58–66.

1116 Wang D et al. 2022. ELOVL gene family plays a virtual role in response to breeding
1117 selection and lipid deposition in different tissues in chicken (Gallus gallus). *BMC*
1118 *Genomics* 23:705.

1119 Widelitz RB et al. 2003. Molecular biology of feather morphogenesis: a testable model
1120 for evo-devo research. *J Exp Zool B Mol Dev Evol* 298:109–122.

1121 Yan X et al. 2022. Functional divergence of the pigmentation gene melanocortin-1
1122 receptor (MC1R) in six endemic Macaca species on Sulawesi Island. *Sci Rep*
1123 12:7593.

Zhang H et al. 2021. Novel mutations in the *Myo5a* gene cause a dilute coat color phenotype in mice. *The FASEB Journal* 35:e21261.

Zhang Y et al. 2017. Acetylation targets HSD17B4 for degradation via the CMA pathway in response to estrone. *Autophagy* 13:538–553.

Zhao C et al. 2023. Detection of CD36 gene polymorphism associated with chicken carcass traits and skin yellowness. *Poult Sci* 102:102691.

Figure Captions

Figure 1. An adult female (left) and an adult male (right) northern cardinal. The adult female is predominately brown in color whereas the adult male has bright red plumage. Photo © Geoffrey E. Hill.

Figure 2. Boxplots of carotenoid concentrations measured from the plasma (left column) and feather follicle (right column) of female (brown) and male (red) northern cardinals. This includes the ketocarotenoids (A, B), non-ketocarotenoid carotenoids (C, D), combined lutein/zeaxanthin representing dietary carotenoids (E, F), and canary xanthophylls (G, H). Significance was assessed according to Welch's two-sample t-test (NS: $p > 0.05$; *: $p <= 0.05$; **: $p <= 0.01$; ***: $p <= 0.001$; ****: $p <= 0.0001$). All values are also indicated with points. The boxes indicate the median, the lower and upper hinges of the boxes correspond to the first and third quartiles, with whiskers extending to the smallest/largest value up to 1.5 times the value of the interquartile range.

Figure 3. Representative high-performance liquid chromatography chromatograms from HEK293 cells transfected with cardinal *CYP2J19*, *BDH1L*, and *TTC39B* and provided with a zeaxanthin (A) or lutein (B) substrate.

Figure 4: Differential gene expression between males and females in the feather follicle (A, B), gut (C) and liver (D). MAplot (A, C, D) with candidate and putative coloration genes labeled. The dashed line on x=0 indicates a log fold change (LFC) of zero and the lighter dashed lines on either side of x=0 indicate LFCs of -0.5 and 0.5, respectively. (B) A volcano plot of the feather follicle gene expression data demonstrating the high significance of the differential expression in the BCO2 gene. The dashed line on the y-axis indicates the significance cutoff of adjusted p=0.05. LFC>0 indicates upregulation in females, whereas LFC<0 indicates upregulation in males. Significantly upregulated genes in males and females are indicated by red and brown dots, respectively.

Figure 5. Gene expression quantification by transcripts per million (TPM) across the feather follicle (left), gut (middle), and liver (right) for the putative carotenoid coloration genes *CYP2J19* (A), and *TTC39B* (B), *BDH1L* (C), and *BCO2* (D), by sex. For clarity, the Y-axis of (D) has been log-transformed. Significance of the difference in read count assessed using independent hypothesis weighting in DESeq2 and significant differences in read count are indicated in bolded asterisks (NS: $p > 0.05$; *: $p <= 0.05$; **: $p <= 0.01$; ***: $p <= 0.001$; ****: $p <= 0.0001$). All values are also indicated with points. The boxes indicate the median, the lower and upper hinges of the boxes correspond to the first and third quartiles, with whiskers extending to either the smallest/largest value or up to 1.5 times the value of the interquartile range.

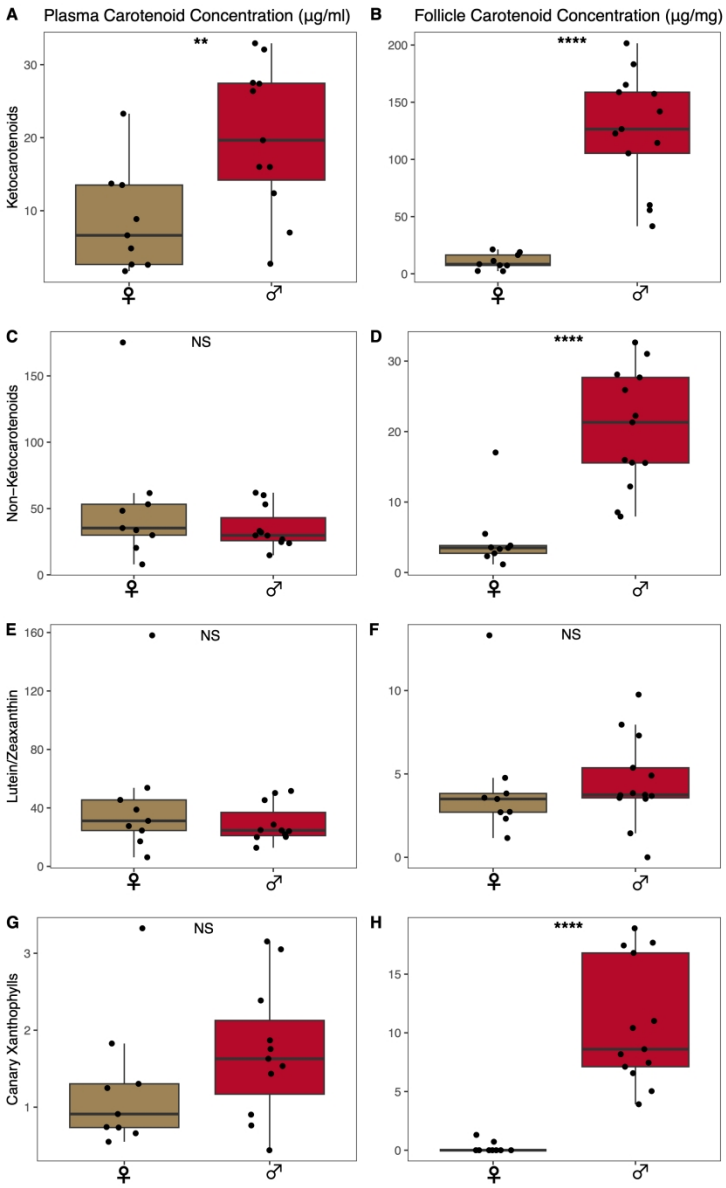

899x1481mm (72 x 72 DPI)

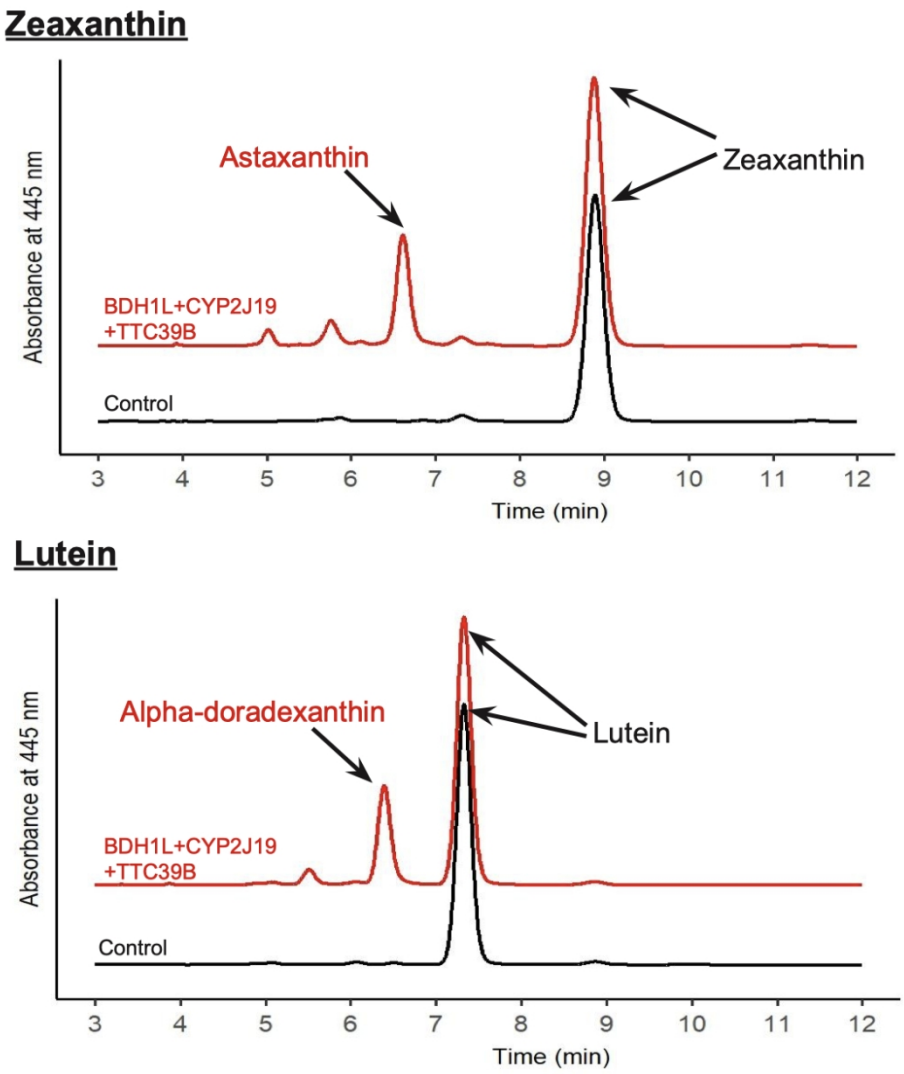

207x226mm (144 x 144 DPI)

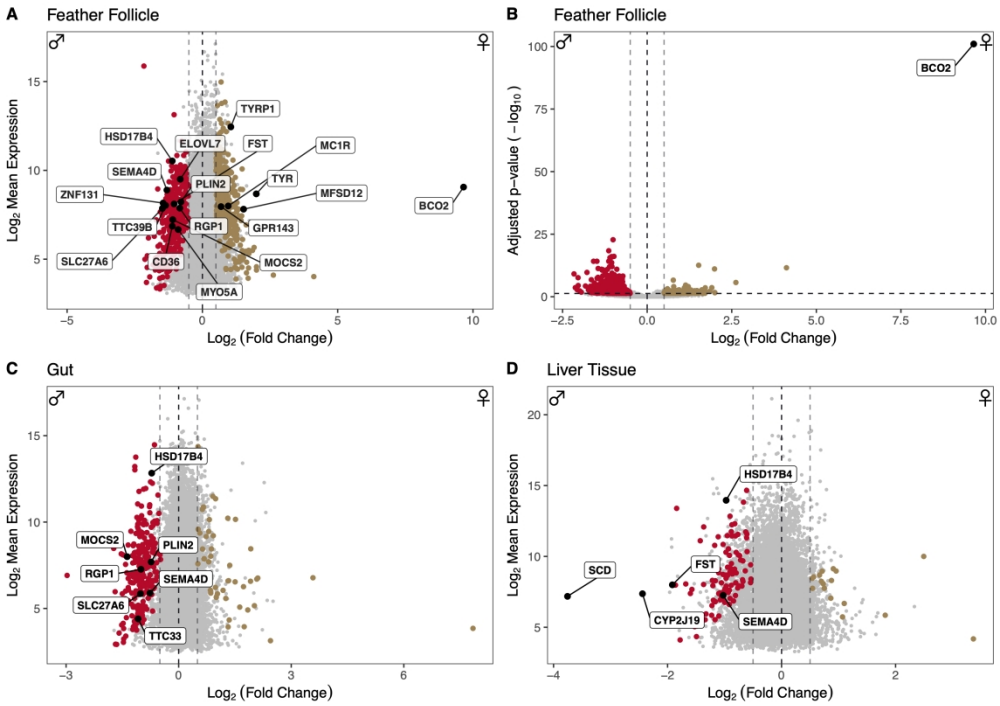

1236x874mm (72 x 72 DPI)

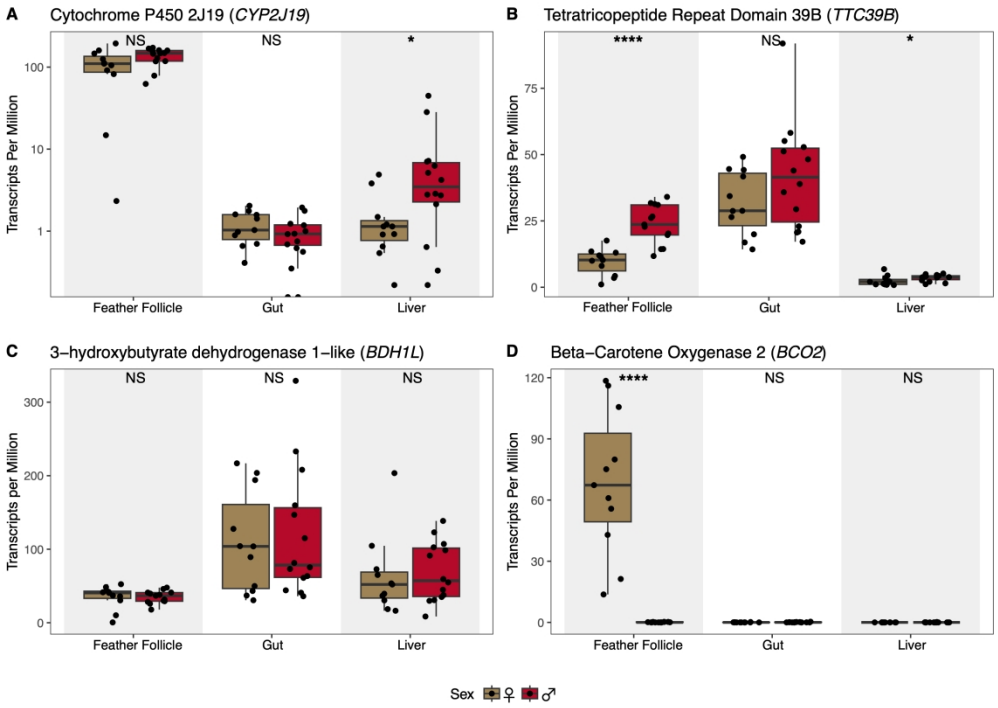

1236x874mm (72 x 72 DPI)